CBPF-NF-035/99

Photofission of ^{27}Al nucleus in the quasi-deuteron region of photonuclear absorption

O. A. P. TAVARES[1], *E. DE PAIVA*[1](*), *G. YA. KEZERASHVILI*[2], *R. YA. KEZERASHVILI*[3], *N. YU. MUCHNOI*[2], *A. I. NAUMENKOV*[2], *I. YA. PROTOPOPOV*[2], *E. A. SIMONOV*[2], *and M. L. TERRANOVA*[4]

[1]Conselho Nacional de Desenvolvimento Científico e Tecnológico - CNPq, Centro Brasileiro de Pesquisas Físicas - CBPF, 22290-180 Rio de Janeiro - RJ, Brazil

[2]Budker Institute of Nuclear Physics - BINP, Siberian Division, Russian Academy of Sciences, 630090 Novosibirsk, Russia

[3]Department of Physics, New York City Technical College, University of New York, Brooklyn, NY 11201, USA

[4]Dipartimento di Scienze e Tecnologie Chimiche, Università di Roma "Tor Vergata", and Istituto Nazionale di Fisica Nucleare - INFN (Sezione di Roma 2), 00133 Roma, Italy

Abstract - Quasi-monochromatic photon beams of 108-MeV Compton-edge energy produced in the ROKK-1M facility at the storage ring VEPP-4M (BINP, Novosibirsk) and makrofol sheets as fission track detectors have been used to measure the photofission yield of ^{27}Al. The fission yield was found (160 ± 55) μb. From the present result and previously measured ^{27}Al photofission yield at $\sim$ 79 MeV end-point energy with the LADON apparatus, the trends of fission cross section and fissility have been obtained in the incident photon energy range $\sim 40 - 110$ MeV. The present results and data for other intermediate-mass nuclei obtained with the same methodolgy have indicated an increase of fissility with decreasing Z^2/A as predicted by the liquid-drop model for fissioning systems lighter than $\sim$ Ag.

(*) Permanent Address : Instituto de Radioproteção e Dosimetria - IRD/CNEN, Av. Salvador Allende s/n, 22780-160 Rio de Janeiro - RJ, Brazil.

E-mail : epaiva@ird.gov.br

Nuclear fission has been intensively investigated during the last sixty years, showing indeed to be a powerful probe to find a number of properties of atomic nuclei as well as to understand the behavior of such nuclei when they are struck by energetic particles and/or photons. In particular, photofission reactions have received much attention from researchers soon after the development of new techniques to produce high-quality monochromatic (or quasi-monochromatic) photon beams of energies greater than $\sim$ 20 MeV, thus allowing to obtain more reliable photofission cross section data [1-22].

On the theoretical side, Myers and Swiatecki [23] developed a nuclear liquid drop model to calculate the height of the fission barrier of nuclei throughout the periodic table, giving values which reach to a maximum of $\sim$ 55 MeV at about the mass region of the nickel-tin nuclei, therefore lighter and heavier nuclei being expected to fission more easily. Estimates of the variation of nuclear fissility throughout the periodic table were obtained for the first time by Nix and Sassi [24], who showed that fissility of nuclei of $Z^2/A \lesssim 20$ does not decrease exponentially with decreasing of Z^2/A, but indeed it increases from a minimum located near silver. This trend has been confirmed later on by Iljinov *et al.* [25], who have used detailed Monte Carlo calculations applied to the cascade-evaporation model of particle- and photon-induced nuclear reactions, and the liquid drop model of fission to obtain a clear trend of increasing fissility with decreasing of Z^2/A for nuclei lighter than silver.

The predict trend of fissility mentioned above has been found experimentally by various authors [26-33], and more recently by Tavares *et al.* [17] and Terranova *et al.* [20,22] in a series of photofission experiments of ^{51}V,^{nat}Ti, and ^{27}Al nuclei at energies in the range $\sim$ 60-145 MeV. The photofissility data resulting from the reported experiments have been very satisfactorily interpreted within the framework of a two-step model for the photofission reaction [17,34]. According to this model the incoming photon is considered to be absorbed by a neutron-proton pair (Levinger's nuclear photoabsorption mechanism [35]), followed by an evaporation-fission competition process for the excited residual nucleus.

Both the theoretical and experimental results reported here have motivated us to con-

duct an additional photofission experiment in ^{27}Al nucleus taking advantage of the photon doses provided by the ROKK-1M facility (BINP, Novosibirsk) and high performance of the fission-track recording method by plastic detectors to record nuclear fragments of relatively low ionization rate [17,20,22]. Another motivation to such an experiment was the observation of a high yield value of ^{11}C from ^{27}Al (much above from the spallation pattern) found long ago in a 1-GeV bremsstrahlung-induced reactions in aluminum targets [36]. The interpretation was that the yield of ^{11}C could be considered near the maximum of a mass-yield curve of the fission of ^{27}Al, i. e., ^{11}C might be likely a fission product from ^{27}Al [37].

Aiming to construct a trend of the photofission cross section and fissility of ^{27}Al nucleus in the energy range $\sim 40-110$ MeV the present photofission yield datum obtained at 108-MeV Compton-edge energy has been combined with the one previously obtained at $\sim$ 79-MeV end-point energy [17] to derive such trends. Results are briefly discussed, and fissility data at 100-MeV incident photon for various target nuclei have been intercompared.

The experiment followed basically the procedures described in detail in our previous papers [20,22]. The samples to be exposed to photon beams consisted of a single stack of 115 metallic $\sim$ 10-μm thick aluminum foils, each one in close contact with a pair of sheets of 145-μm thick makrofol polycarbonate as fission-track recorders. The stack has been exposed to normal incidence of quasi-monochromatic photon beams produced at the ROKK-1M apparatus by Compton backscattering of laser light against the high-energy electrons circulating in the VEPP-4M storage ring.

The experimental arrangement is shown in figure 1, and the main photon-beam characteristics at the ROKK-1M facility have been record as : i) electron energy of 1.8 GeV in the VEPP-4M collider; ii) 2.34 eV for the laser gamma-ray energy; iii) a photon total dose of $(4.0 \pm 0.1) \times 10^9$ measured with a NaI(Tl) photoabsorption callorimeter of threshold energy of 14 ± 2 MeV; iv) 5 % of bremsstrahlung impurity in the photon beam; v)

beam intesity of $\sim 1 \times 10^6$ photons/sec; vi) Compton edge-energy of 108 MeV; vii) energy resolution (FWHM) of $\sim 22\%$; and viii) beam spot at the stack of diameter of $\phi \gtrsim 16$ mm. Figure 2 shows a typical energy spectrum of Compton backscattered γ-beam taken with the NaI(Tl) calorimeter after collimation. During exposure the energy spectrum was continuously monitored by a magnetic pair spectrometer, and coincidences between the signals coming from the NaI(Tl) detector, scintillation counter, and laser pulses have defined the contributions due to Compton and bremsstrahlung photons in the flux, as previously reported in details in Refs. [20,38].

The best etching conditions to produce legible etched fission-like fragment tracks from ^{27}Al (essentially C and N ions of mean ionization rate $-\frac{dE}{dx} \lesssim 1.2$ MeV.μm^{-1}) have been defined as 6.25 N NaOH solution at 70 ^{0}C with gentle stirring. The amount of etching has been fixed such that it produces a thickness of detector removed of $h = (1.48 \pm 0.05)$ μm. Under these etching conditions the mean etch-pit opening of fission fragments from aluminum results to be ~ 3 μm, therefore easy to be differentiated from spurious background by conventional optical microscopy. A total of $n = 64$ detectors (~ 580 cm^2 of total area) has been scanned by one observer (single scanning), and results checked by a second one. Fission track identification and counting have been performed by using Leitz Ortholux microscopies with calibrated eyepieces in 12.5$\times$ oculars, and fitted out with dry objectives of 45$\times$ magnification. Such a procedure enable us to identify tracks of etch-pit opening larger than a minimal of $d = (1.8 \pm 0.1)$ μm. Based on the current scanning methodology and a low track population recorded in the present and previous measurements [15-17], a counting efficiency of $\epsilon_c = (0.79 \pm 0.07)$ has been assumed for track loss during track analysis. Mapping of a total of 127 tracks recorded was constructed from their coordinate positions (fig. 3), which shows the recorded tracks distributed over an approximate circular region of diameter value compatible with that expected from the geometry of irradiation. After background subtraction, the net amount of $N_F = 104 \pm 12$ *fission tracks* has been found in the region of the beam spot.

The photofission yield, Y, represents the sum of all contributions to the total number

of *fission events* produced in target material due to incidence of photons of energy k given by the energy spectrum depicted in fig. 2, and it is defined as

$$Y(k_f) = \frac{N_{fe}}{QN_a} = \int_{k_i}^{k_f} \sigma_f(k)s(k)\mathrm{d}k, \tag{1}$$

where k_i = 14 MeV, k_f = 108 MeV (fig. 2), $\sigma_f(k)$ is the photofission cross section at the energy k, $s\,(k) = \frac{dn}{dk}$ is the energy distribution normalized to one photon in the range $k_i - k_f$, N_{fe} is the number of fission events occurred per unity volume of the target sample, $N_a = 6.0 \times 10^{22}$ cm^{-3} is the number of target nuclei per unity volume, and Q is the total number of incident photons (total dose) per unity area. Since the sample stack contains a large number of target and detector materials the appropriate attenuation of the photon dose throughout the stack has been estimated by the law of exponential decrease of photon beam intensity, under the condition of good geometry of irradiation. In addition, the effect of self-absorption of fission fragments by thick aluminum targets has been also considered to obtain the corrected values of the effective target thickness, x_{eff}, and the average total efficiency, ϵ. These quantities have been evaluated by the method developed in Ref. [39]. Accordingly, under the conditions of the present experiment the photofission yield turns out to be

$$Y = \frac{(N_n/n)}{N_a x_{eff} \epsilon \epsilon_c Q}, \tag{2}$$

with $x_{eff} = (2.1 \pm 0.2)$ μm, $\epsilon = (24 \pm 7)$ %, and $Q = (4.2 \pm 0.1) \times 10^9$, from which values one obtains $Y = (160 \pm 55)$ μb. The final error in the yield value comes from a combination of statistical ($\sim$ 15%) plus systematic ($\sim$ 32%) errors associated with various quantities appearing in (2).

From our previous photofission investigation of pre-actinide and intermediate-mass nuclei with Compton backscattered photon beams [4,6,8,22], and also the photofission experiments in ^{174}Yb and ^{154}Sm nuclei performed with virtual photon spectra by Moretto *et al.* [40], it has been studied the variation of fissility with incident photon energy. Results have been summarized in [22], and they show a general trend of increasing fissility with increasing energy in the quasi-deuteron region of photonuclear absorption. This behavior

has been shown particularly valid for intermediate-mass and less-massive nuclei such as ^{174}Yb,^{154}Sm,^{51}V, and ^{nat}Ti nuclei. Accordingly, fissility data for these target nuclei have been fitted to a general expression of the form

$$f(k) = a(k - B_f)^b, \qquad B_f \lesssim k < 145 \text{ MeV}, \tag{3}$$

where B_f is the height of the fission barrier, and a and b are parameters to be determined from the data. The value for parameter b has been found in the range $1 < b < 2$. Since fissility data for ^{51}V, ^{nat}Ti, and ^{27}Al target nuclei have been obtained with much the same experimental procedure and methodololy [17,20,22, and this work] we assume eq. (3) valid for ^{27}Al too, with $1 < b < 2$. The photofission reactions in the quasi-deuteron region ($\sim 30 - 140$ MeV) have currently been described by means of a two-step model, according to which the reaction begins with the primary photointeraction taking place with a neutron-proton pair and is followed by de-excitation of the resulting residual nucleus by a mechanism in which nucleon emission and fission compete [17,34]. In the case of ^{27}Al target nucleus, the excited residuals which can be formed are ^{26,27}Al and ^{25,26}Mg. Therefore, a nearly symmetric break-up from these residuals are expected to produce the fragment pairs ^{13}C+^{14}N, ^{14}C+^{13}N, ^{13}C+^{13}N, ^{13}C+^{13}C, and ^{12}C+^{13}C, and moreover the less symmetric ones involving ^{11}C, such as ^{11}C+^{16}N, ^{11}C+^{14}N, and others. An estimate of the quantity B_f for ^{27}Al (under the assumption of no excitation energy for the primary fragments) can be found from the average kinetic energy released in fission, $< E_k^t >$, for each fissioning residual [41], and from the Q-value for the corresponding break-up mode of the fissioning system ($B_f \simeq < E_k^t > - \text{Q}$). The $< E_k^t >$-values result in the range $8.8 - 10.1$ MeV, whereas the Q-values (nearly symmetric modes) are found between -36 MeV and -23 MeV. Accordingly, the resulting B_f-values vary in the range $33 - 44$ MeV (the value $B_f \approx 40$ MeV emerges from the liquid drop model [23]). Some excitation energy may also contribute to the final value of B_f, but the amount of excitation should not alter significantly the large interval of the B_f-values as estimated above. Therefore, we write

$$f(k) = a(k - B_f)^b, \quad \begin{cases} B_f < k \lesssim 110 \text{ MeV} \\ 33 \lesssim B_f \lesssim 44 \text{ MeV} \\ 1 < b < 2 \end{cases} \tag{4}$$

to describe the trend of fissility for ^{27}Al nucleus, where the values for parameters a, b, and B_f have been estimated as explained below.

The photofission cross section is calculated by

$$\sigma_f(k) = \sigma_a^T(k) \times f(k), \tag{5}$$

where

$$\sigma_a^T(k) = L\frac{NZ}{A}\sigma_d^f(k)e^{-D/k} \tag{6}$$

represents the total nuclear photoabsorption cross section calculated according to Levinger's modified quasi-deuteron model [42]. Here, $\sigma_d^f(k)$ is the total photodisintegration cross section of the free deuteron [43], $L = 5.6$ is the Levinger's constant for ^{27}Al [44], and $D = 10.4$ MeV is the *damping* parameter-value for ^{27}Al [45]. Next, eq. (1) is used together with expressions $(4-6)$ and the photofission yield-values measured at $k_L = 79$ MeV with the LADON γ-beam ($Y_L = (180 \pm 40)$ μb [17]), and at $k_R = 108$ MeV with the ROKK-1M γ-beam ($Y_R = (160 \pm 55)$ μb [this work]), to give

$$\begin{cases} Y_R = 38a\int_{B_f}^{k_R}\sigma_d^f(k)e^{-D/k}(k-B_f)^b s_R(k)\,\mathrm{d}k \\ Y_L = 38a\int_{B_f}^{k_L}\sigma_d^f(k)e^{-D/k}(k-B_f)^b s_L(k)\,\mathrm{d}k, \end{cases} \tag{7}$$

where $s_R(k)$ and $s_L(k)$ are the normalized photon energy spectra measured at the ROKK-1M and LADON facilities, respectively. The system of equations (7) has solutions for values of parameters a, b, and B_f within the constraints defined in (4) provided that $Y_R/Y_L > 1$, which condition is not verified in the present case. However, the condition $Y_R/Y_L > 1$ can be eventually satisfied if one observes the large errors associated with both Y_R and Y_L measurements (the Y_R/Y_L-ratio is indeed affected by $\sim 40\%$ of uncertainty). Therefore, by fixing the range $1.16 - 1.24$ for the Y_R/Y_L-values (which range is within the large errors referred above), numerical calculations have been performed by varying the values of parameters b and B_f within the constraints defined in (4). Such calculations have shown that system (7) is satisfied for the average parameter-values (energies in MeV) $a = (7 \pm 2) \times 10^{-4}$, and $b = 1.20 \pm 0.08$, if the value 37 MeV is assumed for the height of the fission barrier. These have been used in equation (4) to obtain the fissility values. The uncertainty associated with the f -values comes from a combination of the errors of

parameters a and b. Figure 4 shows the resulting trends of σ_f (part b) and f (part c), as well as their respective uncertainties (shady areas). It is deduced, for instance, that fissility increases from $(2.5 \pm 0.8) \times 10^{-3}$ at 40 MeV up to $(1.2 \pm 0.5) \times 10^{-1}$ at 110 MeV. To allow a comparison, also shown in fig. 4 are the data obtained at the average incident photon energy of 69 MeV (filled circles) as reported in [17]. These data-points show, within the reported uncertainty, good agreement with the present results.

Finally, in fig. 4-a is depicted the σ_a^T-curve (full line) as calculated by eq. (6), which trend shows to compare satisfactorily well with the measured values by Ahrens *et al.* [46] in the range $\sim 40 - 105$ MeV. Figure 4 summarizes, to our view, the main experimental features of the photofission and photofissility of ^{27}Al nucleus in the range $\sim 40 - 110$ MeV which can be attained by photon sources at our disposal and the current fission-track detection method. Although the present ^{27}Al photofission experiment does not allow to get information on the mass-yield distribution, the reported results are seen not incompatible either with the excess-yield (~ 100 μb) of ^{11}C above the spallation pattern measured at 1-GeV bremsstrahlung [36] or the mean fissility-value (~ 0.12) obtained in the photon-energy range $0.8 - 1.8$ GeV [32].

In concluding the discussion, we represent in fig. 5 a plot of fissility versus parameter Z^2/A at 100-MeV incident photons for various target nucleus. Data taken with Compton backscattered photons at the ROKK-1M facility (filled circles from [22] and open circle from this work), and with virtual photons (filled triangles from [40]) are shown to remark a strong variation of fissility with Z^2/A. On the right side ($Z^2/A > 22$) in fig. 5 an exponential decreasing of f with decreasing nuclear mass is clearly noted, whereas for lighter nuclei ($Z^2/A < 13$) fissility shows to increase again. This behavior is consistent with the predictions from the fission-evaporation competition mechanism of nuclear reactions and the liquid drop model of fission as has been discussed to some detail in [17]. We point out that such results can be interpreted as an inverse reflection of the trend of the height of the fission barrier along the periodic table.

In summary, the present work describes a photon-induced fission experiment in ^{27}Al

nucleus carried out with quasi-monochromatic, backscattered photon beams of 108-MeV Compton-edge energy in which a stack containing a large number of metallic aluminum foils sandwiched between plastic makrofol sheets has been used to detect fission events. From the present and previous [17] photofission yield measurements the trends of fission cross section and fissility have been deduced in the incident photon energy range of $\sim 40-110$ MeV. Both these quantities have shown increase monotonously with increasing energy. On the other hand, fissility data at 100-MeV incident photon energy for a number of pre-actinide, intermediate-mass, and less-massive nuclei have been intercompared showing evidence for an increase of fissility with decreasing Z^2/A in the region of nuclei lighter than about zinc, being compatible with the current models for intermediate-energy photofission reactions [17,21,34]. Of course a phenomenological, semi-empirical analysis of the present results is to be done in order to better evidence the main features of nuclear fissility in the energy region of quasi-deuteron photoabsorption.

***

The authors would like to express their gratitude to the Budker Institute of Nuclear Physics-BINP (Novosibirsk) for supporting the present work. Thanks are due to the experimental staff of the storage ring VEPP-4M and to the technical group of the ROKK-1M facility for providing high-quality photon beams. Partial support by the Brazilian CNPq and the Italian INFN (Sezione di Roma 2) is also gratefully acknowledged.

---

[1] LEMKE H. -D., ZIEGLER B., MUTTERER M., THEOBALD J. P. and CÂRJAN N., *Nucl. Phys.*, **A342** (1980) 37.

[2] BELLINI V., EMMA V., LO NIGRO S., MILONE C., PAPPALARDO G. S., DE SANCTIS E., DI GIACOMO P., GUARALDO C., LUCHERINI V., POLLI E. and REOLON A. R., *Nuovo Cimento,* **36** (1983) 587.

[3] AHRENS J. *et al., Phys. Lett.*, **B146** (1984) 303.

[4] RIES H. *et al., Phys. Lett.*, **B139** (1984) 254.

[5] BELLINI V. *et al., Nuovo Cimento,* **85A** (1985) 75.

[6] LEPRÊTRE A. *et al., Nucl. Phys.*, **A472** (1987) 533.

[7] LO NIGRO S. *et al., Nuovo Cimento,* **98A** (1987) 643.

[8] GUARALDO C. *et al., Phys. Rev. C*, **36** (1987) 1027.

[9] LUCHERINI V. *et al., Phys. Rev. C*, **39** (1989) 911.

[10] BERNABEI R., DE OLIVEIRA V. C., MARTINS J. B., TAVARES O. A. P., PINHEIRO FILHO J. D., D'ANGELO S., DE PASCALE M. P., SCHAERF C. and GIROLAMI B., *Nuovo Cimento,* **100A** (1988) 131.

[11] MARTINS J. B. *et al., Nuovo Cimento,* **101A** (1989) 789.

[12] MARTINS J. B., MOREIRA E. L., TAVARES O. A. P., VIEIRA J. L., CASANO L., D'ANGELO A., SCHAERF C., TERRANOVA M. L., BABUSCI D. and GIROLAMI B., *Phys. Rev. C*, **44** (1991) 354.

[13] IVANOV D. I., KEZERASHVILI G. YA., L' VOV A. I., MISHNEV S. I., NEDOREZOV V. G., PROTOPOPOV I. YA. and SUDOV A. S., *Yad Fiz.*, **55** (1992) 3 [Engl. Transl. : *Sov. J. Nucl. Phys.*, **55** (1992) 1].

[14] ILJINOV A. S., IVANOV D. I., MEBEL M. V., NEDOREZO V. G., SUDOV A. S., and KEZERASHVILI G. YA., *Nucl. Phys.*, **A539** (1992) 263.

[15] TAVARES O. A. P. *et al., Phys. Rev. C*, **44** (1991) 1683.

[16] TAVARES O. A. P. *et al., J. Phys. G : Nucl. Part. Phys.*, **19** (1993) 805.

[17] TAVARES O. A. P. *et al., J. Phys. G : Nucl. Part. Phys.*, **19** (1993) 2145.

[18] BIANCHI N. *et al., Phys. Lett.*, **B299** (1993) 219.

[19] BIANCHI N. *et al., Phys. Rec.*, **48** (1993) 1785.

[20] TERRANOVA M. L. *et al., J. Phys. G : Nucl. Part. Phys.*, **22** (1996) 511.

[21] TERRANOVA M. L., KEZERASHVILI G. YA., KISELEV V. A., MILOV A. M., MISHNEV S. I., PROTOPOPOV YA., ROTAEV V. N, SHATILOV D. N. and TAVARES O. A. P., *J. Phys. G : Nucl. Part. Phys.*, **22** (1996) 1661.

[22] TERRANOVA M. L. *et al., J. Phys. G : Nucl. Part. Phys.*, **24** (1998) 205.

[23] MYERS W. D. and SWIATECKI W. J., *Nucl. Phys.*, **81** (1966) 1.

[24] NIX J. R. and SASSI E., *Nucl. Phys.*, **81** (1966) 61.

[25] ILJINOV A. S., CHEREPANOV E. A. and CHIGRINOV S. E., *Yad Fiz.*, **32** (1980) 322 [Engl. Transl. : *Sov. J. Nucl. Phys.*, **32** (1980) 166].

[26] METHASIRI T. and JOHANSSON S. A., *Nucl. Phys.*, **A167** (1971) 97.

[27] KASILOV V. I., MITROFANOVA A. V., RANYUK YU. N. and SOROKIN P. V., *Hochenergie Atomkernphysik*, **6** (1973) 8.

[28] CABÔT C., NGÔ C. PÉTER J. and TAMAIN B., *Nucl. Phys.*, **A244** (1975) 134.

[29] KIELY F. M., PATE B. D., HANNAPE F. and PÉTER J., *Z. Phys. A*, **279** (1976) 331.

[30] EMMA V., LO NIGRO S. and MILONE C., *Nucl. Phys.*, **A257** (1976) 438.

[31] DAVID P., DEBRUS J., FAHLBUSCH H. and SCHULZE J., *Nucl. Phys.*, **319A** (1979) 205.

[32] DE LIMA D. A., MARTINS J. B. and TAVARES O. A. P., *Nuovo Cimento,* **103A** (1990) 701.

[33] TERRANOVA M. L., PINHEIRO FILHO J. D., DE ALMEIDA E. S., MARTINS J. B. and TAVARES O. A. P., *Nuovo Cimento,* **104A** (1991) 1429.

[34] TAVARES O. A. P. and TERRANOVA M. L., *Z. Phys.,* **A343** (1992) 407.

[35] LEVINGER J. S., *Phys. Rev.,* **84** (1951) 43.

[36] DI NAPOLI V., SALVETTI F., TERRANOVA M. L., DE CARVALHO H. G. and MAR-

TINS J. B., *Phys. Rev. C*, **8** (1973) 206.

[37] FULMER C. B., TOTH K. S., WILLIANS I. R., HANDLEY T. H., DELL C. F., CALLIS E. L., JENKINS T. M. and WYCKOFF J. M., *Phys. Rev. C*, **2** (1970) 1371.

[38] KEZERASHVILI G. YA., MILOV A. M., MUCHNOI N. YU. and USOV A., *Proc. XIII Panic* (Perugia), edited by PASCOLINI A. (Singapore : World Scientific), vol. II (1993) 839; KEZERASHVILI G. YA. *et al., High Energy Spin Physics, Proc. XI Int. Symp. (Bloomington)*, edited by HELLER K. J. and SMITH S. L. (Woodbury, N. Y. : AIP), vol. 343 (1995) 360.

[39] TAVARES O. A. P., *Nucl. Tracks Radiat. Meas.*, **21** (1993) 239.

[40] MORETTO L. G., GATTI R. C., THOMPSON S. G., ROUTTI J. T, HEISENBERG J. H., MIDDLEMAN L. M., YEARIAN M. R. and HOFSTADTER R., *Phys. Rev.*, **179** (1969) 1176.

[41] TAVARES O. A. P. and TERRANOVA M. L., *Nuovo Cimento A,* **105** (1992) 723.

[42] LEVINGER J. S., *Phys. Lett.,* **82B** (1979) 181.

[43] ROSSI P., *Phys. Rev. C*, **40** (1989) 2412.

[44] TAVARES O. A. P. and TERRANOVA M. L., *J. Phys. G : Nucl. Part. Phys.*, **18** (1992) 521.

[45] TERRANOVA M. L., DE LIMA D. A. and PINHEIRO FILHO J. D., *Europhys. Lett.*, **9** (1989) 523.

[46] AHRENS J., BORCHERT H., CZOCK K. H., EPPLER H. B., GIMM H., GUNDRUM H., KRÖNING M., RIEHN P., SITA RAM G., ZIEGER A. and ZIEGLER B., *Nucl. Phys.*, **A251** (1975) 479.

Figure Captions

Fig. 1 - Experiment set-up of the ROKK-1M facility at the storage ring VEPP-4M (BINP, Novosibirsk, Russia). L1 is a focusing lens; M1 and M2 are mirrors; C is a circular collimator of 8 mm in diameter and 10 cm of lead; CM is a cleaning magnet; SC is a scintillation counter; T + D is the stack of aluminum targets and makrofol detectors; PC is a proportional chamber with 2 mm lead converter; NaI(Tl) is a total photoabsorption calorimeter of 10cm $\times$ 10cm $\times$ 40 cm for gamma-beam spectrometry and dose measurements.

Fig. 2 - Energy distribution (normalized to one photon) of the ROKK-1M photon beam taken with the NaI(Tl) calorimeter after collimation.

Fig. 3 - Mapping of fission tracks recorded on the detector surface obtained from a stack of 64 makrofol sheets. The circle represents the beam spot region $\phi \sim 19$ mm).

Fig. 4 - Total nuclear photoabsorption cross section, σ_a^T, phofission cross section, σ_f, and nuclear fissility, f, as a function of photon energy, k, for ^{27}Al nucleus. Experimental data : ■, σ_a^T as measured by Ahrens *et al.* [46]; •, Ref. [17]. The curves represent the trends described by equations (6) (part a), (5) (part b) and (4) (part c); shady areas indicate the uncertainties associated with σ_f and f.

Fig. 5 - Nuclear fissility at 100-MeV incident photon as a function of Z^2/A of the target nucleus. Experimental data : ▲, ^{174}Yb and ^{154}Sm from Ref. [40]; •, ^{209}Bi,^{nat}Pb,^{197}Au,^{nat}Pt,^{nat}W,^{181}Ta,^{51}V, and ^{nat}Ti from Ref. [20]; O ^{27}Al (this work); the dashed lines are simply to guide the eyes.

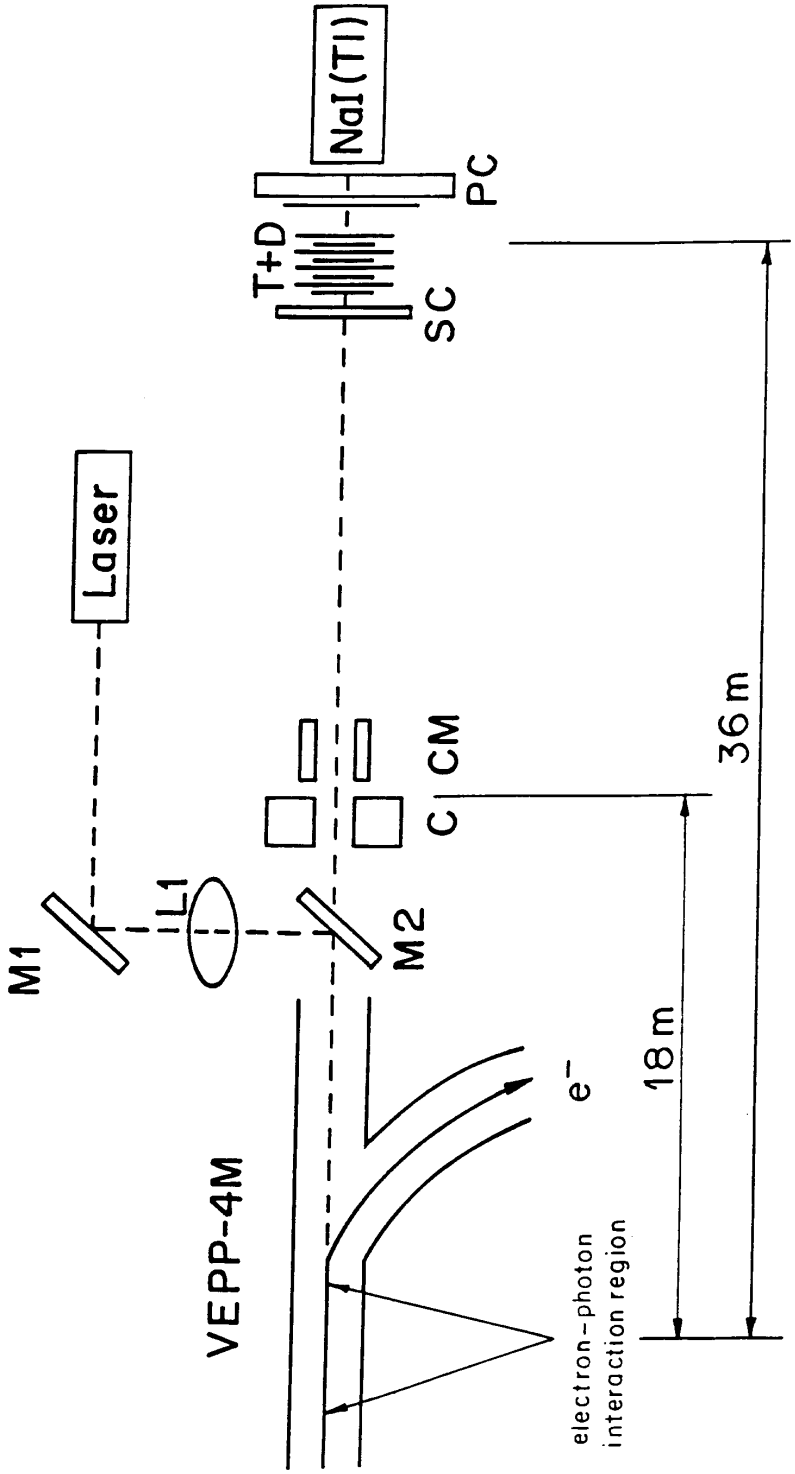
NaI(Tl)
PC
T+D
SC
Laser
CM
36 m
M1
L1
M2
18 m
e⁻
VEPP-4M
electron-photon
interaction region

FIG. 1.

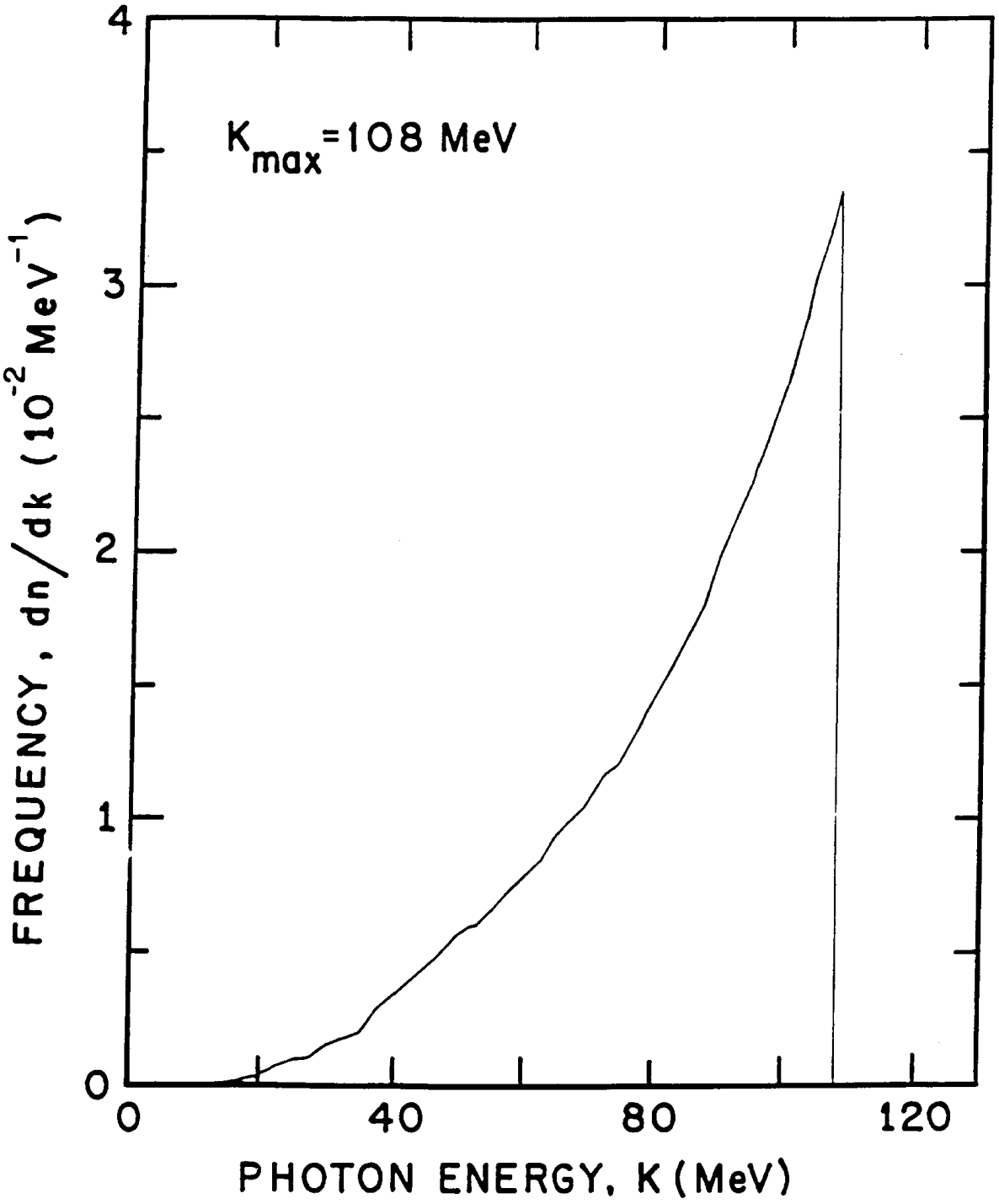
K_{max}=108 MeV
FREQUENCY, dn/dk (10^{-2} MeV^{-1})
PHOTON ENERGY, K (MeV)
0
1
2
3
4
0
40
80
120

FIG. 2.

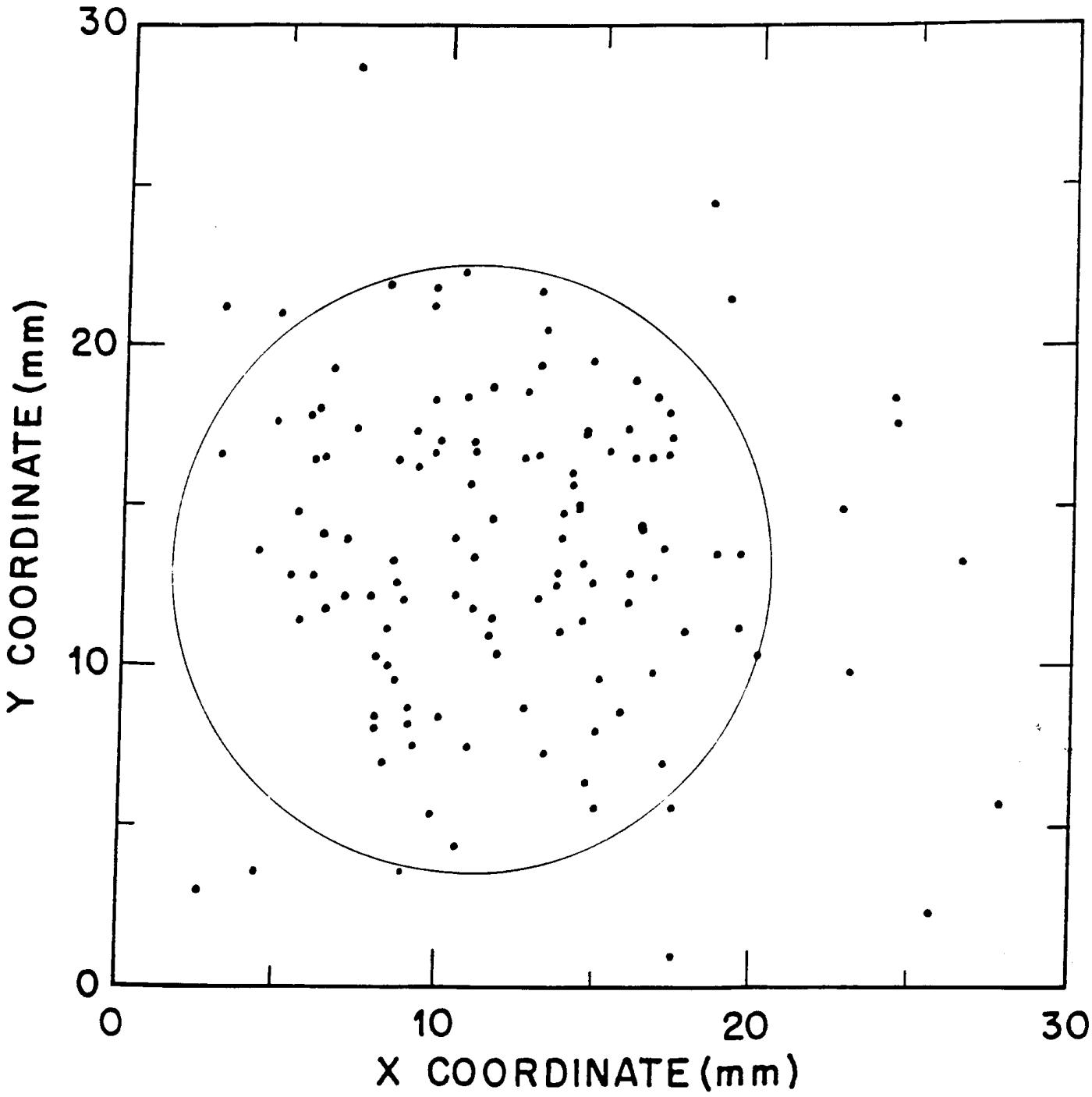

FIG. 3.

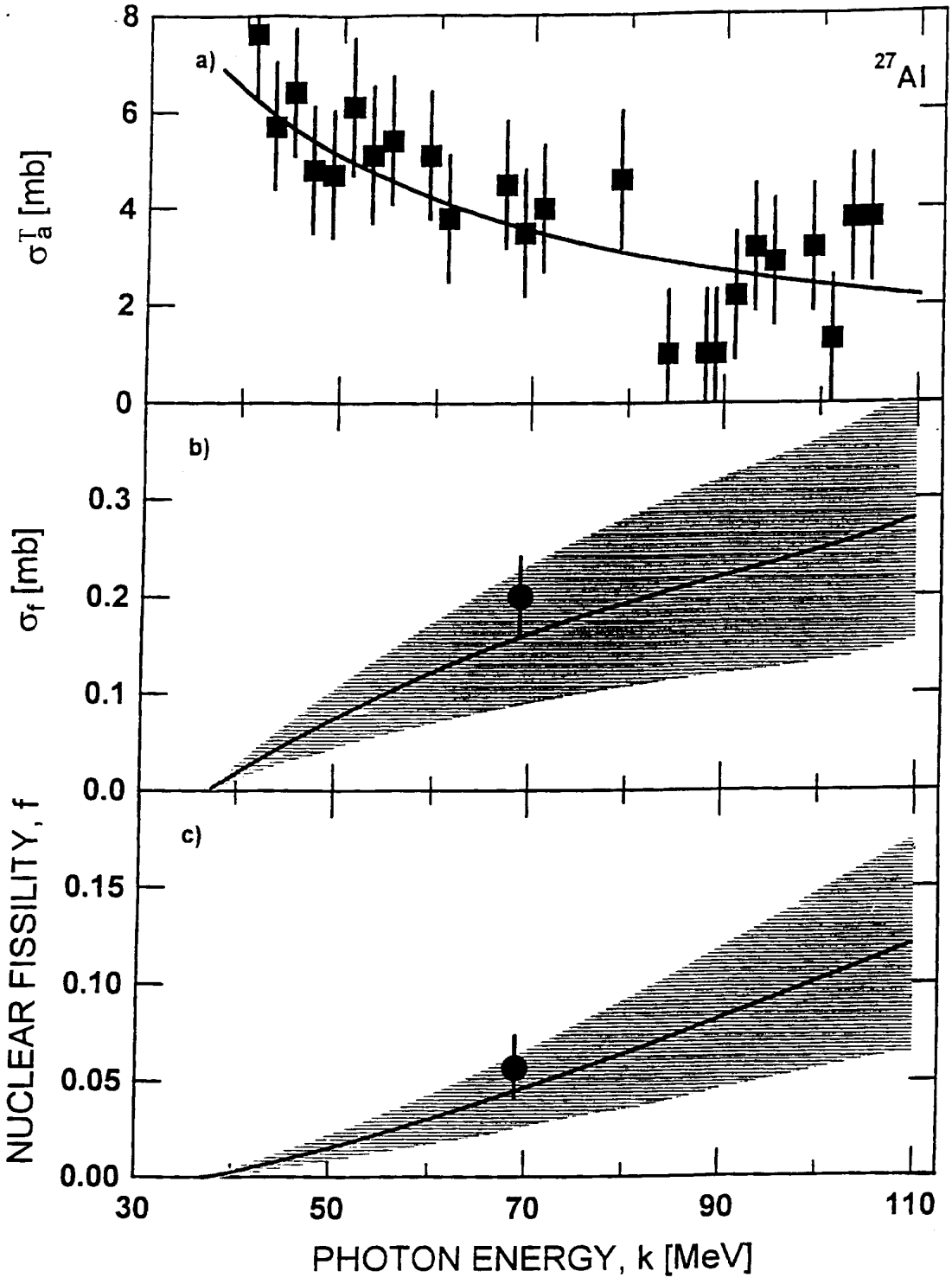
a)
^{27}Al
σ_a^T [mb]
8
6
4
2
0
b)
σ_f [mb]
0.3
0.2
0.1
0.0
c)
NUCLEAR FISSILITY, f
0.15
0.10
0.05
0.00
30
50
70
90
110
PHOTON ENERGY, k [MeV]

FIG. 4.

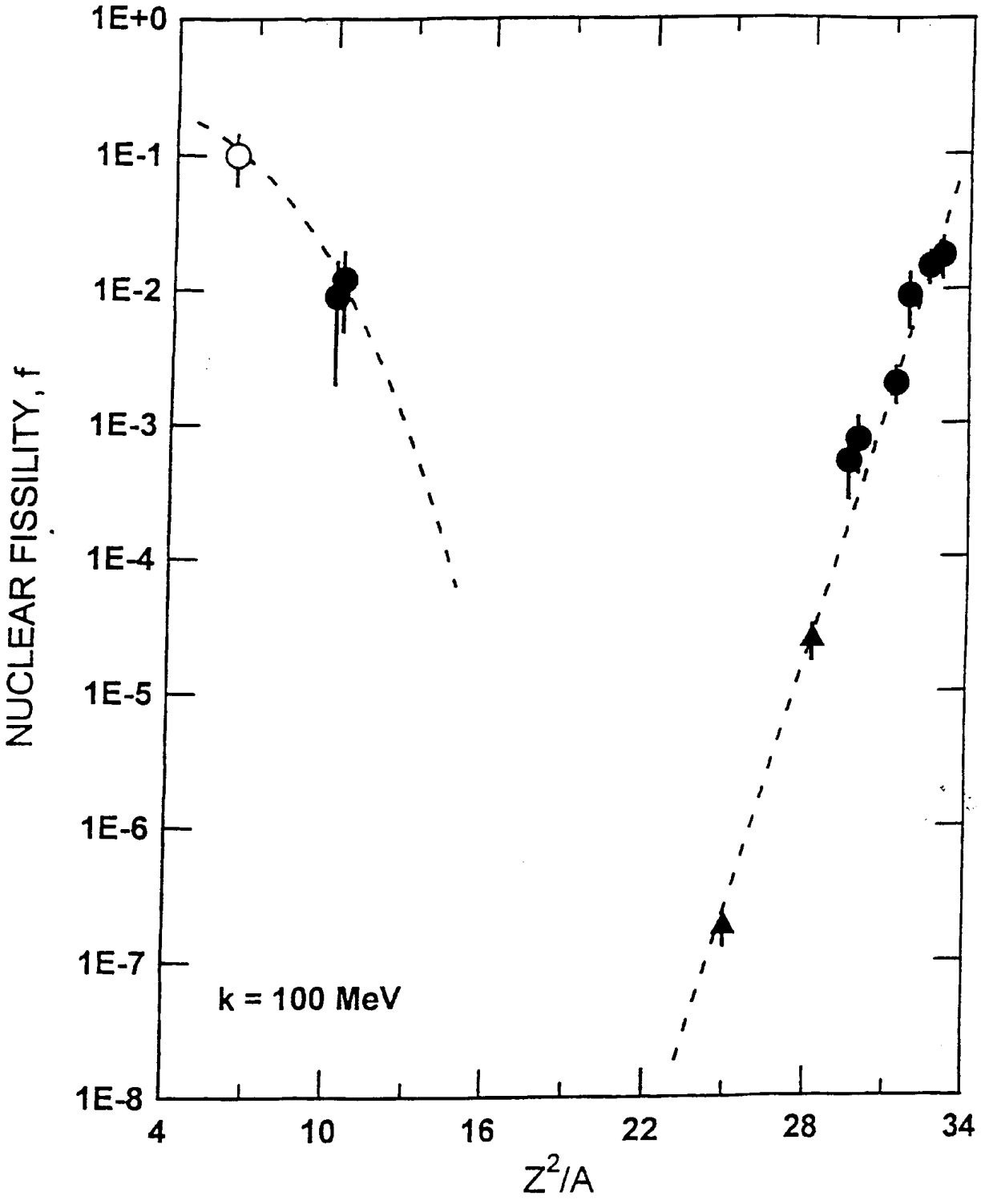
1E+0
1E-1
1E-2
1E-3
1E-4
1E-5
1E-6
1E-7
1E-8
NUCLEAR FISSILITY, f
k = 100 MeV
4
10
16
22
28
34
Z²/A

FIG. 5.